

# An Assay to Detect Protection of the Retinal Vasculature from Diabetes-Related Death in Mice

Yanliang Li<sup>1</sup>, Andrius Kazlauskas<sup>1,2</sup>

<sup>1</sup> Department of Ophthalmology and Visual Sciences, University of Illinois at Chicago <sup>2</sup> Department of Physiology and Biophysics, University of Illinois at Chicago

## Corresponding Author

Andrius Kazlauskas

ak20@uic.edu

## Citation

Li, Y., Kazlauskas, A. An Assay to Detect Protection of the Retinal Vasculature from Diabetes-Related Death in Mice. *J. Vis. Exp.* (2023), e66123, doi:10.3791/66123 (2024).

## Date Published

January 12, 2024

## DOI

10.3791/66123

## URL

jove.com/video/66123

## Abstract

Diabetic retinopathy (DR) is a complex and progressive ocular disease characterized by two distinct phases in its pathogenesis. The first phase involves the loss of protection from diabetes-induced damage to the retina, while the second phase centers on the accumulation of this damage. Traditional assays primarily focus on evaluating capillary degeneration, which is indicative of the severity of damage, essentially addressing the second phase of DR. However, they only indirectly provide insights into whether the protective mechanisms of the retinal vasculature have been compromised. To address this limitation, a novel approach was developed to directly assess the retina's protective mechanisms - specifically, its resilience against diabetes-induced insults like oxidative stress and cytokines. This protection assay, although initially designed for diabetic retinopathy, holds the potential for broader applications in both physiological and pathological contexts. In summary, understanding the pathogenesis of diabetic retinopathy involves recognizing the dual phases of protection loss and damage accumulation, with this innovative protection assay offering a valuable tool for research and potentially extending to other medical conditions.

## Introduction

Diabetic retinopathy (DR) is one of the microvascular complications of diabetes mellitus (DM), and the leading cause of blindness in working-age individuals in developed countries<sup>1</sup>. Major risk factors for diabetic retinopathy are the duration and degree of hyperglycemia<sup>2,3,4</sup>. While DM causes dysfunction of both the vascular and neural

components of the retina<sup>5</sup>, diagnosis of DR is based on morphological features of the retinal vasculature<sup>6</sup>.

Hyperglycemia-induced oxidative stress is one of the drivers of DR pathogenesis<sup>7</sup>. Increased oxidative stress causes widespread damage, which compromises the functionality of the mitochondria and thereby further increases the level of reactive oxygen species. These events are accompanied

by leakage of retinal vessels, an increase in the level of inflammatory cytokines, and death of both neural and vascular cell types within the retina. Loss of vascular cells, and hence the functionality of the extensive capillary network of the retina, results in hypoxia, a potent stimulus for a variety of responses<sup>5</sup>. Such responses include increased expression of vascular endothelial growth factor (VEGF) that drives both permeability and angiogenesis, cardinal features of the advanced, sight-threatening stages of DR - diabetic macular edema, and proliferative diabetic retinopathy<sup>6</sup>.

Certain features of DR suggest that an organism (both patients and experimental animals) has an intrinsic ability to resist this indication. Patients experience several decades of DM before they develop sight-threatening DR<sup>8,9,10,11,12,13</sup>. While rodent models of DM do not develop the advanced, sight-threatening stages of DR<sup>14</sup>, the initial/mild form of DR that manifests does so only after a period of weeks or months of DM<sup>15,16</sup>. Furthermore, in both patients and experimental animals, DR is progressive, and retinal dysfunction/damage increases as the duration of DM is prolonged. Finally, some patients with DM never develop DR. In certain instances, this is because such individuals do not experience diabetes long enough for DR to develop. In other instances, it is because they display extraordinary resistance to DR; as is the case with participants of the Medalist study, who do not develop DR after 50 or more years of DM<sup>17</sup>. Despite such compelling support for the existence of protection from DR and its enormous translational relevance, the mechanism underlying protection has not been aggressively investigated.

The protection assay described herein was developed to facilitate investigation of why DR is delayed from the onset of DM in diabetic mice. The key steps of this assay, applied

to DM and non-DM mice, include (1) delivering a sub-maximal death-inducing insult to the eye (*ex vivo* or *in vivo*), (2) isolating the retinal vasculature, (3) staining the vasculature with TUNEL and DAPI, (4) photographing the resulting images and quantifying the percentage of TUNEL/DAPI double-positive species.

## Protocol

All animal studies were approved by the Office of Animal Care and Institutional Biosafety at the University of Illinois at Chicago. Seven-week-old male C57/BL6/J mice were housed in group cages in a pathogen-free environment on a 12 h-light/dark cycle and provided free food and water access. Mice were euthanized by CO<sub>2</sub> asphyxiation, and the eyes were enucleated and processed immediately<sup>18</sup>. The animals were obtained from a commercial source (see **Table of Materials**). The essential tools needed for the study are depicted in **Figure 1**.

### 1. Delivery of the death-inducing insult

1. Perform oxidative stress with TBH (*ex vivo*).
  1. Euthanize the mice following institutionally approved protocols and enucleate their eyes<sup>18</sup> (**Figure 2A**).
  2. Put the eyeballs directly into individual wells of a 24-well plate containing DMEM + 1% BSA, with or without 5 mM Tert-butyl hydroperoxide (TBH) (see **Table of Materials**); incubate for 1 h at 37 °C. A positive control sample is treated with DNase (50 U/100 µL) for 10 min to fragment DNA.
 

**NOTE:** The dose of TBH (the agent that induces oxidative stress) was chosen to induce a readily detectable and sub-maximal level of cell death within the isolated retinal vessels<sup>18</sup>.

3. Fix the eyes in 10% buffered formalin overnight (16 h minimum).
2. Use cytokine cocktail to induce inflammation (*in vivo*).
  1. Anesthetize the mice with an intraperitoneal injection of 100 mg/kg ketamine and 5 mg/kg xylazine.
  2. Use a customized 33 G needle (see **Table of Materials**) to inject 1  $\mu$ L/eye of the cytokine cocktail into the vitreous; the injection site is 2-3 mm from the limbus (**Figure 2B**).

**NOTE:** The cytokine cocktail contains 1:1:1 ratio of 1  $\mu$ g/mL TNF- $\alpha$ , 1  $\mu$ g/mL IL-1 $\beta$  and 1500 U/ $\mu$ L IFN- $\gamma$ <sup>18</sup> (see **Table of Materials**).

3. 24 h after the injection, euthanize the mice (following institutionally approved protocols), enucleate their eyes and fix with 10% buffered formalin overnight.

**NOTE:** The experiment can be paused after fixation for 1 week maximum and then restarted later.

## 2. Retina isolation

1. Cut open the eyeball.
  1. Use straight forceps to grab the optic nerve gently (**Figure 2C**). Hold a micro-knife with the other hand to make an incision of 2-3 mm posterior to the limbus.
  2. Switch from the micro-knife to micro-scissors to cut parallel to the limbus while rotating the eyeball along with the optic nerve until the eyeball has been cut into two halves.
  3. Discard the anterior half of the eye, including the lens (**Figure 2C**).
2. Remove the sclera.

1. Use straight forceps to gently lift the sclera 1-3 mm off of the retina.
2. Use micro-scissors to make two radial cuts in the sclera part of the way to the optic nerve. Avoid cutting the underlying retina.
3. Use a pair of curved forceps to grab the scleral flap and tear it off the retina. The RPE layer will come off with the sclera.
3. Wash the retina.
  1. Use a micro-spatula to transfer the isolated retina to a well within a 24-well dish that has been filled with double-distilled water.
  2. Gently shake the dish at mid-moderate speed at room temperature. Change the water every 30 min to 1 h, at least 4-5 times, then leave overnight.

## 3. Retinal vasculature isolation

1. Digestion: Replace the double-distilled water with 800  $\mu$ L of YL trypsin solution (3% trypsin in 0.1 M Tris buffer (pH 7.8)). Incubate at 37 °C with gentle to no shaking for 4 h 15 min<sup>19</sup> (**Figure 2D**).
 

**NOTE:** Avoid rapid shaking as this can damage the vasculature.
2. Transfer: Dip the broad end of a glass transfer pipet with YL trypsin solution to transfer the retina to a 35 mm Petri dish containing lint-free, double-distilled water.
3. Remove the outer nuclear layer (photoreceptors) (**Figure 2E**).
  1. Flip the retina semi-sphere downward facing. Use the straight single-hair brush to gently press the retina to the bottom of the dish.

2. Use the loop brush to gently brush away the photoreceptors of the retina. The brush strokes are applied in a direction from the optic nerve towards the periphery of the retina. The photoreceptors can detach in large sheets because they are not anchored to the rest of the retina by blood vessels.
3. Using a 200  $\mu$ L pipette to collect and discard the sheets of neural tissue.
4. Remove the vitreous.
  1. Flip the retina semi-sphere so that it faces upward. Use a pair of curved forceps (A) to grasp the vitreous as much as possible under a dissecting microscope. **NOTE:** The vitreous look like a sheet of transparent tissue attached to the optic nerve or retina.
  2. Use another curved forceps (B) to grasp the end of the vitreous where it connects the optic nerve. Remove the vitreous by pulling forceps A away from forceps B.
  3. Discard the vitreous. Examine the remnant of the vitreous and repeat this step to remove all the vitreous as the residual will impede the next steps.
5. Remove the remaining neural and glial tissue (**Figure 2F**).
  1. Flip the retina semi-sphere so that it is downward facing again. Once again, use the straight brush to gently press the retina to the bottom of the dish (do not use the tip of the hair).
  2. Use the loop brush to gently brush over the vasculature from the optic nerve head towards the periphery to remove the remaining neural tissue<sup>20</sup>.
  3. Spin the retina slowly with the straight brush and use the loop brush to remove all the small chunks

of neural tissue on the retinal vasculature, till the vascular network is well cleaned (**Figure 2G,H**).

#### 4. Mounting the isolated retinal vasculature on a microscope slide

1. Place a microscope slide.
  1. Place a clean mounting cassette (see **Table of Materials**) under a dissecting microscope. Fill the cassette with double-distilled water.
  2. Use a black background under the dissecting microscope to help generate contrast to see the illuminated transparent vasculature.
  3. Use forceps to place a clean, labeled microscope slide into the bottom of the mounting cassette.
2. Transfer the retinal vasculature.
  1. Dip the broad end of a glass transfer pipet with YL trypsin solution.
  2. Transfer the cleaned retinal vasculature and gently dislodge the vasculature into the double-distilled water within the mounting cassette and above the microscope slide.
3. Mount the retinal vasculature.
 

**NOTE:** While the vasculature is floating above the microscope slide, the isolated vasculature will acquire its normal bowl shape.

  1. Use the loop brush to flip the retina semi-sphere facing upward and gently push the vasculature down onto the glass slide, and then use the hair to tack down the opened vasculature onto the center of the slide. The vasculature should stick to the slide as it touches.

2. Flat mount the vasculature by brushing the bowl-shaped retinal vessel from the optic nerve to the periphery.
3. Repeat brushing in all directions till the vasculature sticks to the slide completely.
4. Air dry the retinal vasculature.
  1. Once the entire retinal vasculature attaches to the slide, take the slide out of the water either by gently lifting one edge or by slowly draining water at the corner of the cassette to minimize currents, then pulling it out (**Figure 2I**).
  - NOTE:** The vasculature will become readily visible once it has once air-dried (**Figure 2J**).
  2. Mark the circumference of the retinal vasculature on the back of the slide with a marker pen.
  3. Proceed to stain the sample without pause.
4. Rinse the slide 3 times with PBS to remove the TUNEL reaction mixture. Dry the area around the sample.
5. Add a drop of DAPI mounting media to stain the nuclei with DAPI and mount the sample with a cover glass. Store at 4 °C in the dark.
 

**NOTE:** The protocol could be paused for up to 1 week before capturing images.
6. Photograph the resulting vasculature with a confocal fluorescence microscope (see **Table of Materials**). Capture six to eight randomly selected fields in the far periphery surrounding the optic nerve (**Figure 4**).
 

**NOTE:** Representative images of cytokine-induced apoptotic bodies in isolated retinal vessels are illustrated in **Figure 5**.
7. Analyze the results.
  1. For *ex vivo*, TBH-treated samples, perform the following steps.
    1. Count the number of apoptotic bodies (TUNEL/DAPI double-positive species) in each field using Image J (see **Table of Materials**). Tally the mean of the apoptotic bodies in all of the fields of a single sample.
    2. Calculate the fold change in the number of apoptotic bodies between a randomly selected pair of non-DM and DM samples.
    3. Determine if there is a statistically significant difference using the two-tailed student t-test<sup>18</sup>.
 

**NOTE:** Stain the control and experimental samples (non-DM and DM) on the same occasion because the extent of TUNEL staining can vary, even when done in the same way. Since up to 10 retinas can be cleaned and

## 5. Death detection with TUNEL staining

**NOTE:** For details on this procedure, refer to Zheng et al.<sup>21</sup>. Representative images of ischemia +/- ox stress-induced apoptotic bodies in isolated retinal vessels are depicted in **Figure 3**.

1. Rehydrate the isolated vasculature with PBS. Rinse it 3 times in PBS and then incubate with 1% Triton X-100 in PBS for 2 min on ice to permeabilize the isolated vasculature.
2. Rinse the slides twice with PBS to remove the residual Triton X-100. Dry the area around the sample.
3. Add 50 µL of TUNEL reaction mixture (see **Table of Materials**) onto the sample. Incubate the slide in a humidified atmosphere for 60 min at 37 °C in the dark.

mounted per day by an experienced user, plan to process an equal number of control and experimental retinas before starting this protocol.

2. For *in vivo*, cytokines cocktail treated samples, perform the following the steps.
  1. Manually count the number of apoptotic bodies (TUNEL/DAPI double-positive species) in the entire retinal vasculature.
  2. Calculate the fold change in the number of apoptotic bodies between a randomly selected pair of non-DM and DM samples.
  3. Determine if there is a statistically significant difference using the two-tailed student t-test.

## Representative Results

The successful isolation of retinal vasculature results in a flat mount of the entire network of the mouse retinal vasculature, with the architectural integrity intact (**Figure 2J**). Upon staining with periodic acid-schiff hematoxylin (PASH), it is possible to distinguish the two vascular cell types: endothelial cells (ECs) and pericytes (PCs) (**Figure 6**). The endothelial cell nuclei are elongated, lightly stained, and reside entirely

within the vessel walls. Pericyte nuclei are circular, densely stained, and protrude from the capillary walls. The PASH-stained samples also reveal acellular capillaries, which lack nuclei.

The approach to induce death was guided by the following rationale. It was speculated that protection was limited, i.e., could be overwhelmed by a very strong death-inducing insult. Consequently, insults (both ischemia/oxidative stress and cytokines<sup>18</sup>) were optimized so that they would induce a readily detectable increase but yet submaximal extent of death (**Figure 3** and **Figure 5**).

It is important to highlight that the presence of TUNEL-positive nuclei was contingent on the specific type of insult employed to trigger cell death. The ischemia/oxidative stress insult led to a tram-track pattern of cell apoptosis, as illustrated in **Figure 3**, whereas the cytokine insult resulted in a distinct and well-defined pattern, as depicted in **Figure 5**. Both patterns can be observed in retinal vessels from DR patients<sup>22</sup>, suggesting that both types of agents induce cell death in humans. Moreover, the observed morphological distinctions offer a means to evaluate if pathology was driven by oxidative stress or cytokines.



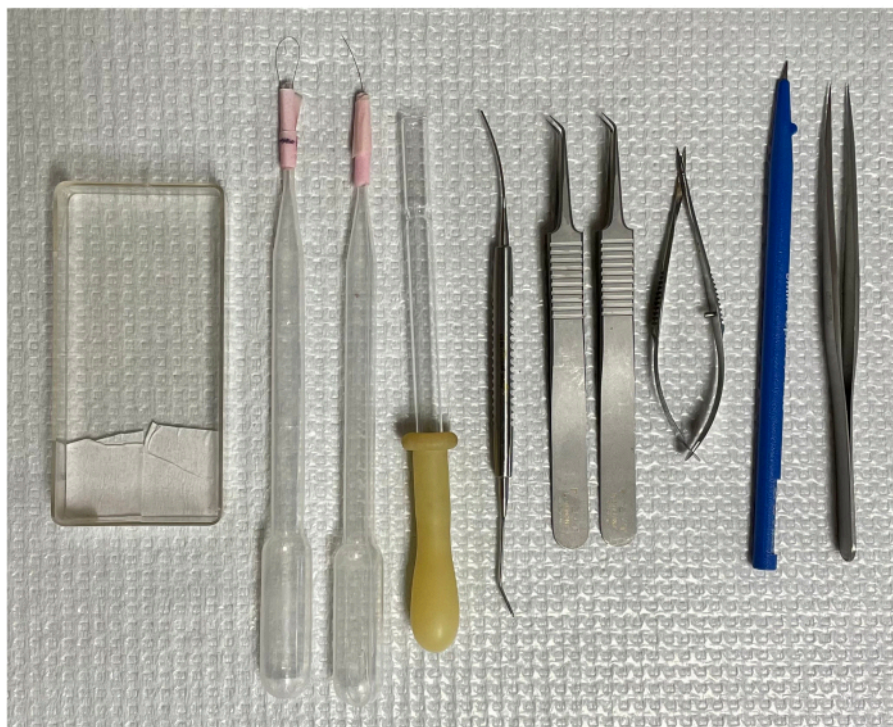


**Figure 1: Tools for isolating mouse retinal vasculature.** From left to right: the mounting cassette, two single-hair brushes, an inverted transfer pipet, micro-spatula, two curved forceps, spring scissors, micro-knife, and forceps with straight tips.

[Please click here to view a larger version of this figure.](#)

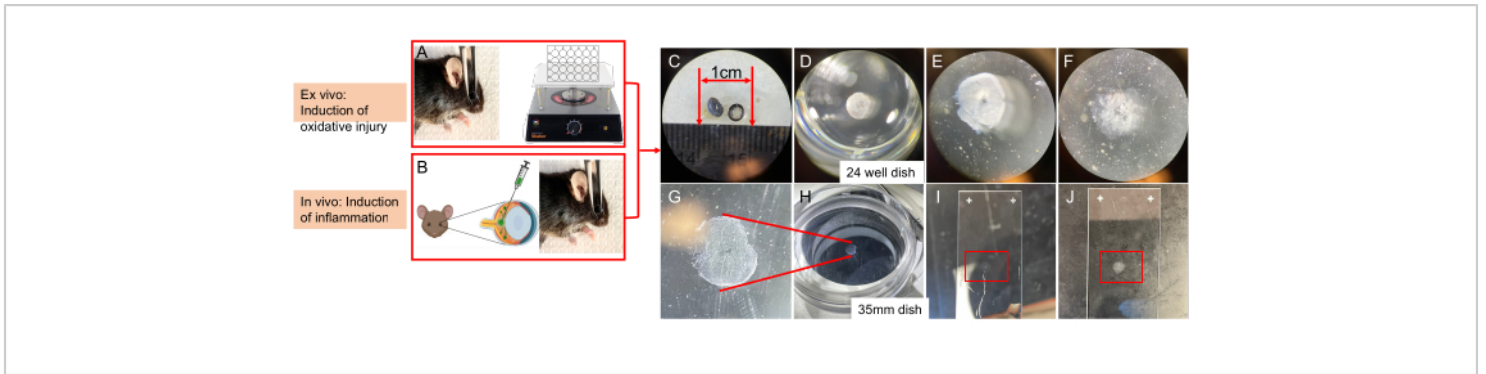


**Figure 2: Schematic showing the key steps of delivering a death-inducing insult and then isolating the retinal vasculature from a mouse eye.** (A) Induction of ischemia/oxidative injury, *ex vivo*. After enucleation, the eyeball is subjected to ischemia in the presence of TBH. (B) *In vivo* administration (intravitreal injection) of cytokines. (C) Cutting the eyeball into two halves. (D) Retinal enzymic digestion: removing the sclera and washing the retina in double-distilled water overnight. Incubating in YL trypsin solution at 37 °C for 4 h 15 min in a well of a 24-well plate. (E) Removing the photoreceptors. (F) Removing the remaining neural and glial tissue. (G) Cleaned bowl-shaped vascular network facing upward. (H) Isolated vascular network in a 35 mm dish with a black background on the stage of a dissecting microscope. (I) Flat-mounted retinal vasculature on a slide. (J) Air-dried retinal vasculature on a slide. This figure has been modified from Li et al.<sup>18</sup>. [Please click here to view a larger version of this figure.](#)



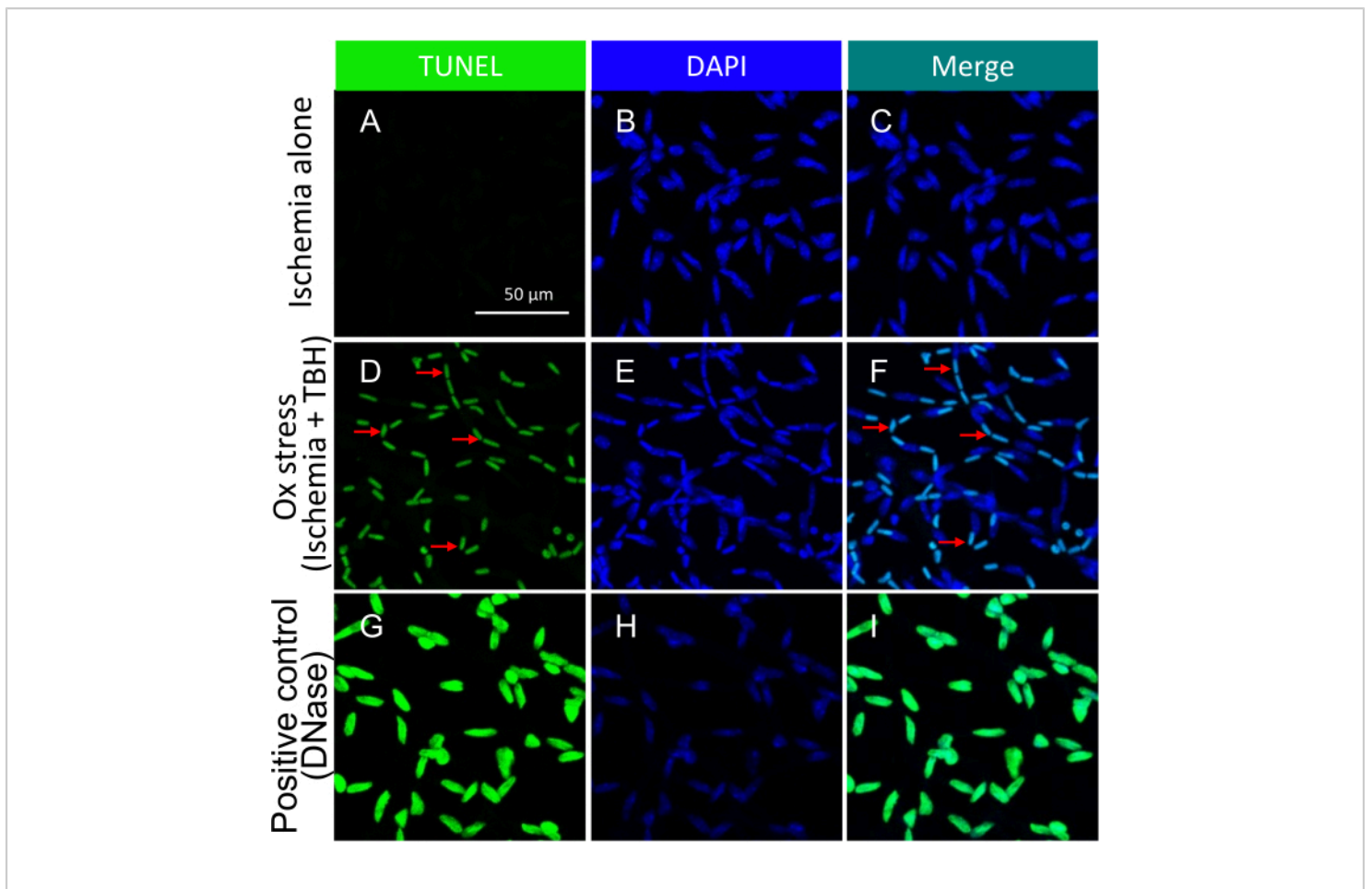


**Figure 3: Detection of apoptotic bodies within mouse retinal vessels treated *ex vivo* with ischemia +/- TBH.**

Representative images of ischemia +/- ox stress-induced apoptotic bodies in isolated retinal vessels. The heading of each column indicates the staining. **(A-C)** Retinal vessels isolated from eyeballs that underwent 1 h of ischemia alone. **(D-F)** Same as **(A-C)**, except the 1 h insult was a combination of ischemia and oxidative stress (5 mM TBH). The red arrows point to representative TUNEL/DAPI double-positive species. **(G-I)** Positive control treated with DNase. Scale bar = 50 μm. This figure has been modified from Li et al.<sup>18</sup>. [Please click here to view a larger version of this figure.](#)

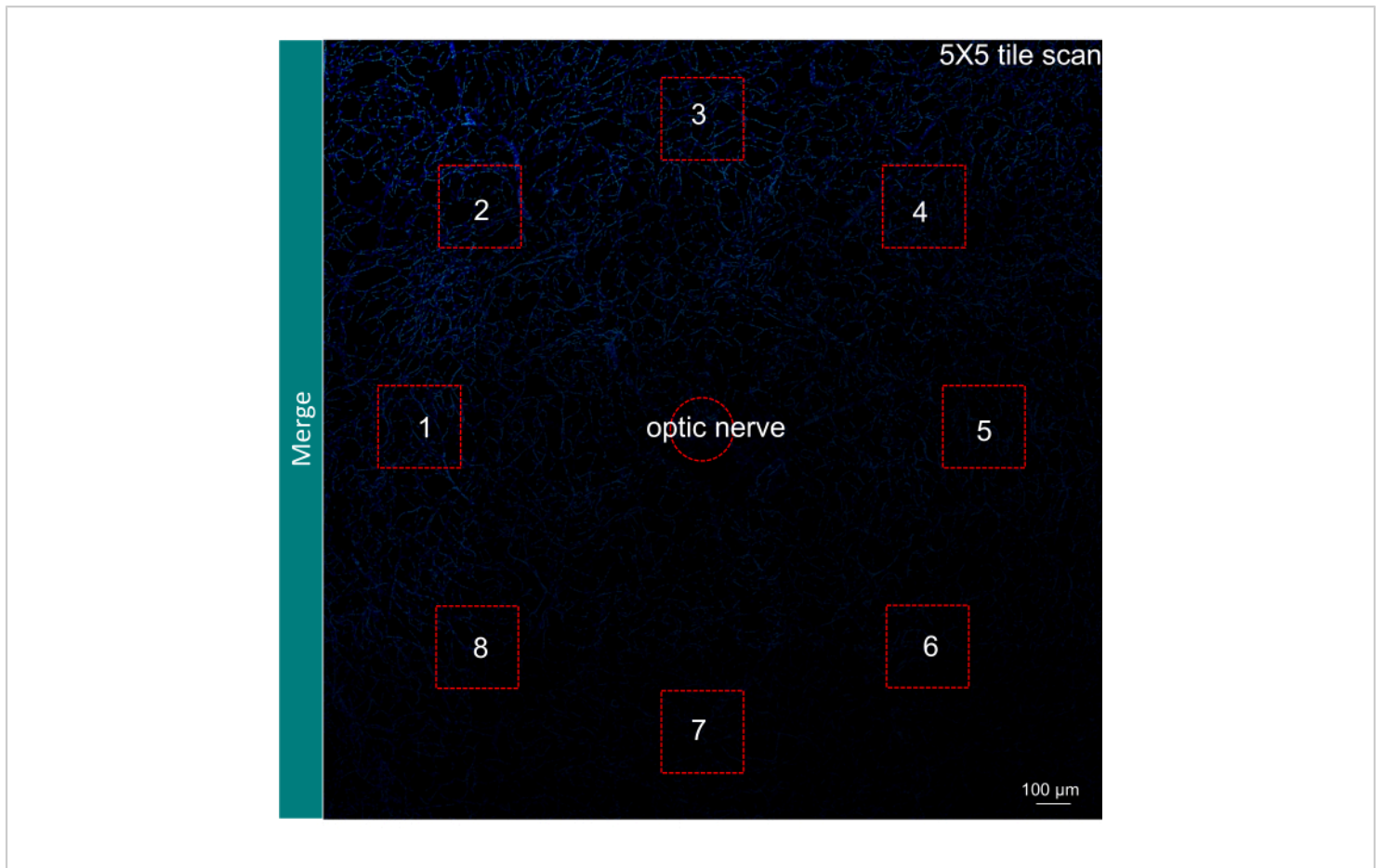


**Figure 4: Illustration of field selection for quantification of results.** A 5 x 5 tile scan of the retinal vasculature with the merge of TUNEL and DAPI signal. The selection of six to eight fields in the far periphery surrounding the optic nerve is shown with red squares. Magnification, 200x. Scale bar = 100  $\mu$ m. [Please click here to view a larger version of this figure.](#)

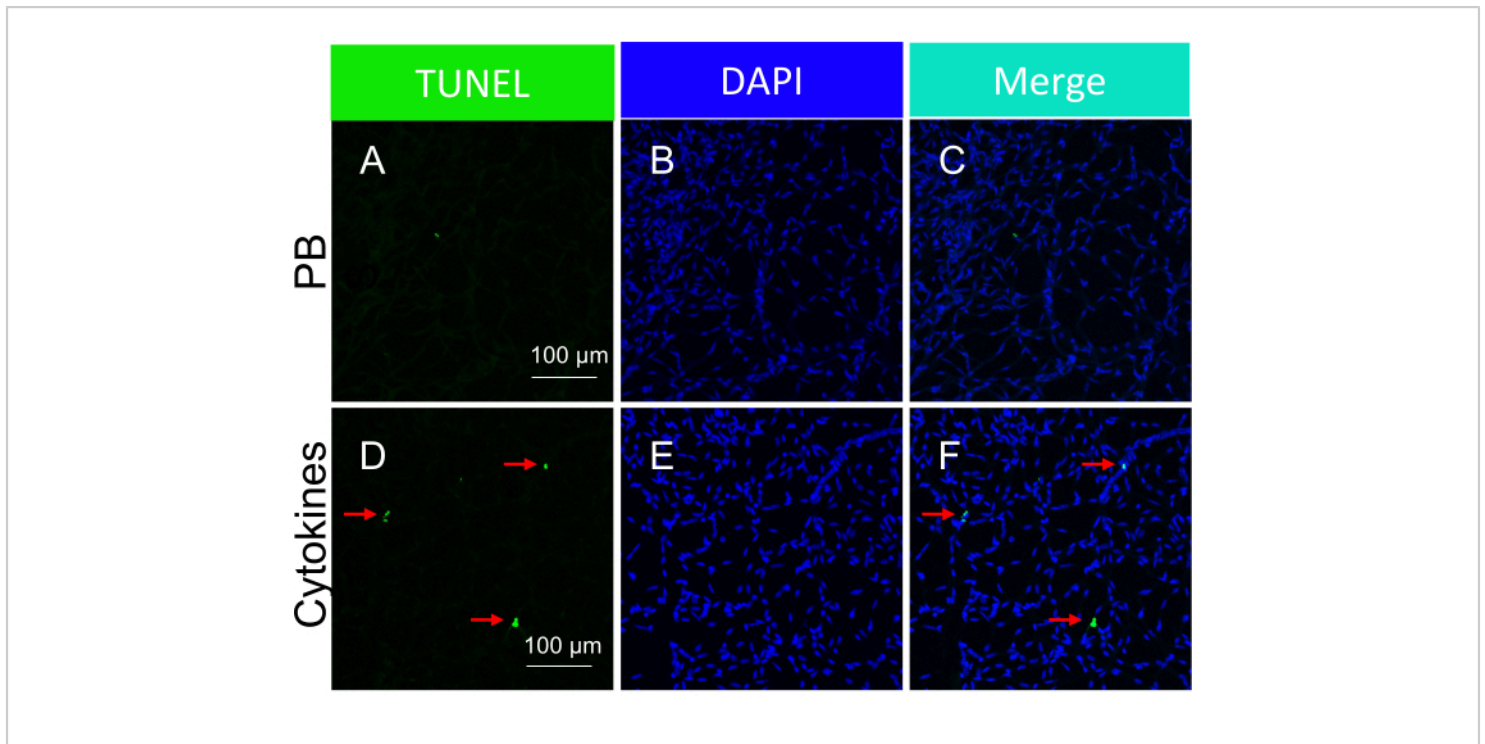


**Figure 5: Detection of the apoptotic bodies within mouse retinal vessels in response to intravitreal injection of cytokines (*in vivo* administration).** Representative images of cytokine-induced apoptotic bodies in isolated retinal vessels. The heading of each column indicates the staining. **(A-C)** Images of the retinal vessels isolated from mice intravitreally injected with PBS. **(D-F)** Same as **(A-C)**, except a cytokine cocktail was injected along with PBS. The red arrows point to representative TUNEL-positive species. Scale bars = 100  $\mu$ m. This figure has been modified from Li et al.<sup>18</sup>. [Please click here to view a larger version of this figure.](#)

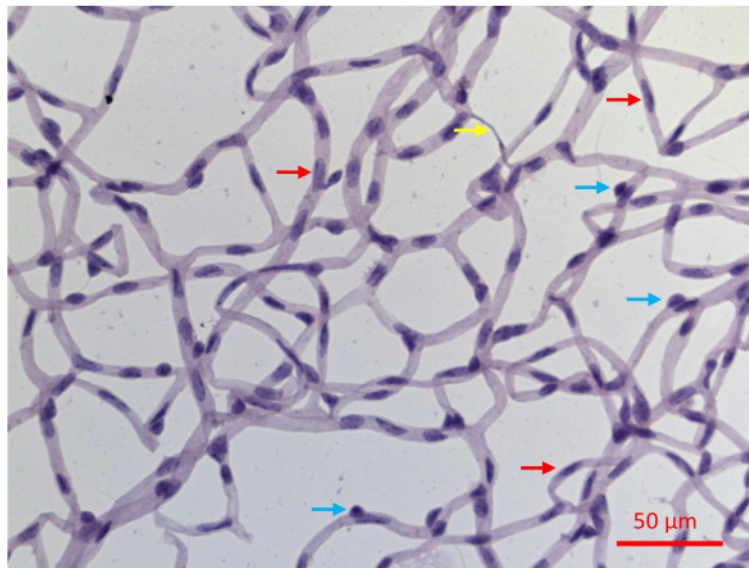


**Figure 6: A representative image of a PASH-stained retinal vessels.** Retinal vessels of a mouse that experienced 20 weeks of STZ-induced DM were isolated as described in **Figure 2**, stained with PASH, and imaged while illuminated with visible light. Pericyte nuclei in capillaries tend to be more circular and densely stained (blue arrows), whereas elongated and less densely stained nuclei are diagnostic of endothelial cells (red arrows). The yellow arrow points to an acellular capillary. Scale bar = 50 μm. [Please click here to view a larger version of this figure.](#)

## Discussion

In this study, an assay was established to detect resistance/vulnerability of the retinal vasculature to death induced by DM/DR-related insults such as ischemia/oxidative stress and cytokines. This manuscript provides a detailed description of this assay, which is a modification of several published protocols<sup>19,20,21</sup>.

The protocol encompasses several crucial stages. First, it is imperative to meticulously dissect the retina, ensuring the preservation of the vascular network and preventing substantial tears. This can be accomplished by making an incision 2-3 mm posterior to the limbus since the retina tightly adheres to the ora serrata, and separating it is challenging. Second, coat all instruments that come into contact with

the vessels (e.g., single-hair brushes, transferring pipet, and forceps) with trypsin by dipping these tools into the YL trypsin solution throughout the procedure. This prevents the vasculature from adhering to the instruments that are used in this protocol. Third, because the microvasculature is nearly invisible under normal light, heightened vigilance is required during debris aspiration and transfer to the microscope slide in order to prevent accidental loss.

An appropriate degree of enzymatic digestion of the various layers of the retina is crucial; insufficient digestion prevents the separation of neuronal tissue from the vascular network, while excessive digestion dissolves the vascular plexus. Various digestion times ranging from 1 h<sup>19</sup> to overnight<sup>23</sup> have been reported. Based on observations, a digestion time

of 4 h and 15 min yields the most favorable results compared to durations of 2 h, 3 h, and 4 h. Prolonging the digestion beyond this point is unlikely to enhance the process and might instead compromise the integrity of the vasculature.

In cases where the digested retina adheres to the single-hair brush, dip the hair in YL trypsin solution multiple times. This reduces the brush's sticky areas. If the hairbrush still adheres to the vascular tissue, then inspect it for residual fragments of vitreous, and remove them with forceps.

The optimal moment for complete vitreous removal is after eliminating the photoreceptors, but prior to the removal of the remaining neural and glial tissue. The retina maintains rigidity until photoreceptors are removed. Extracting the vitreous at this stage could potentially tear the retina/vasculature. The delicate layers of residual neural and glial tissue play a pivotal role in preserving the curved form of the vascular structure. They prevent the retina from tearing at its center when the vitreous is detached from the optic nerve.

If the isolated vasculature does not adhere to the microscope slide at all, then it indicates that the section of the slide where adhesion is expected to occur is dirty. Try moving the vessels across the slide's surface to locate a sticky spot, switching to a different slide or meticulously cleaning the slide and trying again. If the vessels stick to the slide before they unfurl into their bowl-like shape, lift the vasculature from the slide in order to allow it to float freely in the water once again. Do this step with forceps that have been repeatedly dipped in the YL trypsin solution.

Several alternative techniques for isolating the vasculature have been reported, which would not be suitable for the protection assay described herein. For instance, osmotic lysis has been employed to isolate the vasculature from unfixed

retina samples, facilitating biochemical investigations of the tissue<sup>24,25</sup>. However, this procedure may not preserve the anatomy of the vasculature as well as the approach employed in this article. Similarly, while the tissue print method to isolate large segments of microvasculature enables analysis of the vasculature's electrotonic architecture<sup>26</sup>, the entire vascular bed is typically not recovered.

This assay was developed because existing approaches to monitor capillary degeneration do not address the issue of protection. Capillary degeneration, which occurs after prolonged DM, indicates if DR has developed. In addition to diagnosing DR, this outcome is useful to assess if an agent/therapy prevents DR. However, existing capillary degeneration assays do not speak to the underlying mechanism of action of the agent. Such an agent may prevent pathological events that drive DR such as increased oxidative stress or cytokines. Alternatively, the agent may enforce protection by enhancing resilience to oxidative stress and cytokines and/or promote the repair of damage. This new protection assay can be used to determine if the beneficial effect of a given therapy involves enforcing the endogenous system that protects from DM-related death.

A drawback of this protection assay is that it does not distinguish the two cell types within the retinal vessels: endothelial cells (ECs) and pericytes (PCs). While the appearance of their nuclei in PASH-stained sections is cell-type specific (**Figure 6**), not every nucleus displays diagnostic features. Approximately 30% of the nuclei cannot be unambiguously defined as EC or PC at least in part because the two-dimensional images obtained from PASH-stained samples incompletely resolve the three-dimensional structure of the vascular plexus. This obstacle could be surmounted by additional analysis such as immunofluorescent staining with



cell type-specific markers. Such images, which distinguish the two cell types could be co-stained with TUNEL to determine the resistance/vulnerability of each of the vascular cell types.

This vascular-focused assay does not provide any information regarding the neural retina. Additional assays could be developed to provide such information. For instance, instead of isolating the retinal vasculature, a single cell suspension of the entire retina could be generated and then analyzed (by fluorescent activated cell sorting) for resistance/vulnerability. The inclusion of cell type-specific markers (both neural and vascular) along with indicators of cell death would provide a more complete picture of the retinal cell types that have the capacity for protection from DM/DR-mediated death.

In conclusion, the protection assay described herein provides a powerful approach to investigating the mechanism responsible for the delay between the onset of DM and the manifestation of DR in mice.

## Disclosures

The authors have no conflicts of interest to report.

## Acknowledgments

This work was supported by grants from the Illinois Society to Prevent Blindness, National Institute of Health (EY031350 and EY001792) and an unrestricted grant from the Research to Prevent Blindness Foundation.

## References

1. Teo, Z. L. et al. Global prevalence of diabetic retinopathy and projection of burden through 2045: Systematic review and meta-analysis. *Ophthalmology*. **128** (11), 1580-1591 (2021).

2. Lee, R., Wong, T. Y., Sabanayagam, C. Epidemiology of diabetic retinopathy, diabetic macular edema and related vision loss. *Eye Vis (Lond)*. **2**, 17 (2015).
3. Lima, V. C., Cavalieri, G. C., Lima, M. C., Nazario, N. O., Lima, G. C. Risk factors for diabetic retinopathy: A case-control study. *Int J Retina Vitreous*. **2**, 21 (2016).
4. Sabanayagam, C., Yip, W., Ting, D. S., Tan, G., Wong, T. Y. Ten emerging trends in the epidemiology of diabetic retinopathy. *Ophthalmic Epidemiol*. **23** (4), 209-222 (2016).
5. Antonetti, D. A., Silva, P. S., Stitt, A. W. Current understanding of the molecular and cellular pathology of diabetic retinopathy. *Nat Rev Endocrinol*. **17** (4), 195-206 (2021).
6. Wong, T., Cheung, C., Larsen, M., Sharma, S., Simó, R. Diabetic retinopathy. *Nat Rev Dis Primers*. **2**, 16012 (2016).
7. Wu, M. Y., Yiang, G. T., Lai, T. T., Li, C. J. The oxidative stress and mitochondrial dysfunction during the pathogenesis of diabetic retinopathy. *Oxid Med Cell Longev*. **2018**, 3420187 (2018).
8. Hietala, K., Harjutsalo, V., Forsblom, C., Summanen, P., Groop, P. H. Age at onset and the risk of proliferative retinopathy in type 1 diabetes. *Diabetes Care*. **33** (6), 1315-1319 (2010).
9. Aiello, L. P. et al. Diabetic retinopathy. *Diabetes Care*. **21** (1), 143-156 (1998).
10. Klein, R., Klein, B. E., Moss, S. E., Davis, M. D., Demets, D. L. The wisconsin epidemiologic study of diabetic retinopathy. Prevalence and risk of diabetic retinopathy when age at diagnosis is less than 30 years. *Arch Ophthalmol*. **102** (4), 520-526 (1984).



11. Nathan, D. M. et al. The effect of intensive treatment of diabetes on the development and progression of long-term complications in insulin-dependent diabetes mellitus. *N Engl J Med.* **329** (14), 977-986 (1993).
12. Clustering of long-term complications in families with diabetes in the diabetes control and complications trial. The diabetes control and complications trial research group. *Diabetes.* **46** (11), 1829-1839 (1997).
13. Cruickshanks, K. J., Moss, S. E., Klein, R., Klein, B. E. Physical activity and proliferative retinopathy in people diagnosed with diabetes before age 30 yr. *Diabetes Care.* **15** (10), 1267-1272 (1992).
14. Robinson, R., Barathi, V. A., Chaurasia, S. S., Wong, T. Y., Kern, T. S. Update on animal models of diabetic retinopathy: From molecular approaches to mice and higher mammals. *Dis Model Mech.* **5** (4), 444-456 (2012).
15. Samuels, I. S., Bell, B. A., Pereira, A., Saxon, J., Peachey, N. S. Early retinal pigment epithelium dysfunction is concomitant with hyperglycemia in mouse models of type 1 and type 2 diabetes. *J Neurophysiol.* **113** (4), 1085-1099 (2015).
16. Sergeys, J. et al. Longitudinal *in vivo* characterization of the streptozotocin-induced diabetic mouse model: Focus on early inner retinal responses. *Invest Ophthalmol Vis Sci.* **60** (2), 807-822 (2019).
17. Sun, J. K. et al. Protection from retinopathy and other complications in patients with type 1 diabetes of extreme duration: The joslin 50-year medalist study. *Diabetes Care.* **34** (4), 968-974 (2011).
18. Li, Y. et al. The slow progression of diabetic retinopathy is associated with transient protection of retinal vessels from death. *Int J Mol Sci.* **24** (13), 10869 (2023).
19. Chou, J. C., Rollins, S. D., Fawzi, A. A. Trypsin digest protocol to analyze the retinal vasculature of a mouse model. *J Vis Exp.* **76**, e50489 (2013).
20. Veenstra, A. et al. Diabetic retinopathy: Retina-specific methods for maintenance of diabetic rodents and evaluation of vascular histopathology and molecular abnormalities. *Curr Protoc Mouse Biol.* **5** (3), 247-270 (2015).
21. Zheng, L., Gong, B., Hatala, D. A., Kern, T. S. Retinal ischemia and reperfusion causes capillary degeneration: Similarities to diabetes. *Invest Ophthalmol Vis Sci.* **48** (1), 361-367 (2007).
22. Mizutani, M., Kern, T. S., Lorenzi, M. Accelerated death of retinal microvascular cells in human and experimental diabetic retinopathy. *J Clin Invest.* **97** (12), 2883-2890 (1996).
23. Weerasekera, L. Y., Balmer, L. A., Ram, R., Morahan, G. Characterization of retinal vascular and neural damage in a novel model of diabetic retinopathy. *Invest Ophthalmol Vis Sci.* **56** (6), 3721-3730 (2015).
24. Dagher, Z. et al. Studies of rat and human retinas predict a role for the polyol pathway in human diabetic retinopathy. *Diabetes.* **53** (9), 2404-2411 (2004).
25. Podestà, F. et al. Bax is increased in the retina of diabetic subjects and is associated with pericyte apoptosis *in vivo* and *in vitro*. *Am J Pathol.* **156** (3), 1025-1032 (2000).
26. Puro, D. G. Retinovascular physiology and pathophysiology: New experimental approach/new insights. *Prog Retin Eye Res.* **31** (3), 258-270 (2012).